Opt Quant Electron (2014) 46:1353–1358
DOI 10.1007/s11082-014-9884-4

Simulations of a graphene excitable laser for spike processing

Bhavin J. Shastri · Mitchell A. Nahmias · Alexander N. Tait · Paul R. Prucnal

Received: 13 September 2013 / Accepted: 24 January 2014 / Published online: 22 February 2014

Abstract We propose and simulate a novel excitable laser employing passively Q-switching with a graphene saturable absorber for spike processing. Our approach combines the picosecond processing and switching capabilities of both linear and nonlinear optical device technologies to integrate both analog and digital optical processing into a single hardware architecture capable of computation without the need for analog-to-digital conversion. We simulate the laser using the Yamada model—a three-dimensional dynamical system of rate equations—and show behavior that is typical of spiking processing algorithms simulated in small circuits of excitable lasers.

Keywords Computing · Excitability · Graphene · Laser · Mixed-signal · Neural networks · Q-switching · Saturable absorber · Spike processing

1 Introduction

Excitability is a nonlinear dynamical mechanism underlying all-or-none responses to small perturbations (Krauskopf et al. 2003) and occurs near certain types of bifurcations of a dynamical system. A system is said to be *excitable* if it is at an attracting equilibrium state, but can be triggered by a small perturbation to produce a large amplitude excursion, after which the system settles back to the attractor in what is called the *refractory phase*. Excitability is a critical property of spiking networks. Spike processing algorithms are well understood in a number of important biological sensory processing systems and are finding growing use in signal processing applications (Maass and Bishop 1999). Spiking signals encode information as *events* in time (rather than bits). Since the time at which a spike occurs is analog, while its amplitude is digital, this hybrid scheme can exhibit the efficiency of analog computation and the noise robustness of digital computation (Sarpeshkar 1998). Exploiting the high speed, high bandwidth, and low crosstalk available to photonic interconnects, networks of spiking

B. J. Shastri (✉) · M. A. Nahmias · A. N. Tait · P. R. Prucnal
Princeton University, Princeton, NJ 08544, USA
e-mail: shastri@ieee.org

lasers could be used to implement high-performance optical reservoir computing (Vandoorne et al. 2008). The potential of excitable lasers to perform temporal logic grants the capacity for complex, ultrafast categorization and decision-making (Tait et al. 2014; Shastri et al. 2013a; Nahmias et al. 2013a). Excitable lasers have recently been demonstrated with a semiconductor saturable absorber (SA) mirrors (SESAMs) (Barbay et al. 2011; Spühler et al. 1999). However, SESAMs have a narrow tuning range, slow recovery time, low optical damage threshold, and complex and costly fabrication systems (Bonaccorso et al. 2010).

In this paper, we simulate and analyze an excitable laser based on passively Q-switching with a graphene SA originally proposed in Shastri et al. (2013a). Graphene is a 2D atomic-scale honeycomb crystal lattice of sp^2-hybridized carbon atoms whose optical properties originate from its linear dispersion near the Fermi energy with massless Dirac fermions. The optical nonlinear saturable absorption of graphene—as a consequence of Pauli blocking—includes the following features: ultrafast operation (recovery time in fs or ps), low saturable absorption threshold (one order of magnitude lower than SESAMs), large modulation depth ($>60\,\%$ for few layered graphene), and wavelength-independent (infrared to visible spectrum) operation with absorption of 2.3 % of light per layer (Bonaccorso et al. 2010). We show that this SA laser—an architecture ubiquitously employed for self-pulsating lasers (Krauskopf et al. 2003)—exhibits excitability near a saddle-node homoclinic bifurcation.

The system described in Barbay et al. (2011) is isomorphic to our own excitable laser system in the sense that one can be transformed into the other through a series of linear variable substitutions. Because of the cavity length and overall size difference (factor of $\sim$1 million), the Barbay system exhibits dynamics that are on the order 1 million times faster than our own. Our system represents a proof-of-concept for newer approaches based on integrated technologies. Although our graphene fiber laser is slow, it possesses properties useful for processing tasks, including temporal integration and pulse thresholding. The Barbay system could also exhibit these same properties if the absorber were made fast via defects or other means, and could form processing networks with a suitable wavelength converter. The dynamics we desire require very fast absorbers, and potentially wavelength-labeled units if we want to use WDM-based networking schemes. Thus, graphene is particularly well-suited for our system as a result of it's wide-band absorption and fast recovery time.

2 Simulation model

Figure 1 illustrates the architecture of the proposed graphene Q-switched excitable laser. A graphene film ($\sim$5 layers) is used to form the SA which is sandwiched between two fiber connectors with a fiber adapter. The graphene-SA is integrated into the 10-m long laser cavity with 1 m long highly doped erbium-doped fiber (EDF) as the gain medium. The EDF is pumped with a 980 nm laser diode (LD) via a 980/1,550 nm wavelength-division multiplexer (WDM). A polarization controller (PC) improves the output pulse stability by maintaining a given polarization state after each round trip. An isolator (ISO) in the laser cavity ensures unidirectional propagation. The 30 % port of an optical coupler provides the laser output at $\sim$1,560 nm. The rest of the cavity consists of single-mode fiber. To induce perturbations to the gain $g(t)$, 1,480 nm pulses—analog inputs from other excitable lasers—are input to the system via a 1,480/1,550 nm WDM.

This excitable system can be characterized with the Yamada model, a three-dimensional dynamical system of rate equations, which describes the behavior of lasers with independent gain and SA sections with an approximately constant intensity profile across the cavity, as follows (Dubbeldam et al. 1999):

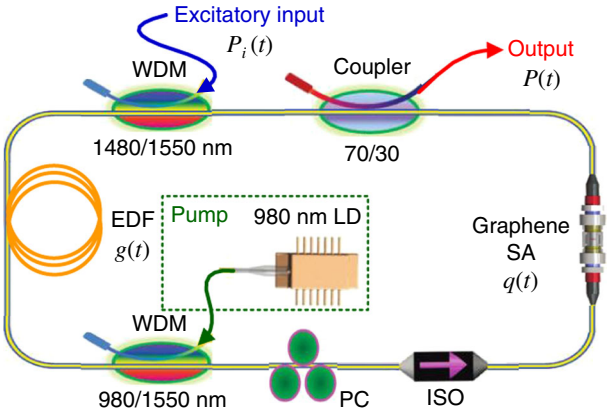

Fig. 1 Architecture of the graphene passively Q-switched excitable laser

$$T_R \frac{dP(t)}{dt} = [g(t) - q(t) - l]\, P(t) \tag{1}$$

$$\frac{dg(t)}{dt} = -\frac{g(t) - g_0}{\tau_L} - \frac{g(t)P(t)}{E_L} + \frac{g(t)P_i(t)}{E_I} + \varepsilon f(g) \tag{2}$$

$$\frac{dq(t)}{dt} = -\frac{q(t) - q_0}{\tau_A} - \frac{q(t)P(t)}{E_A} \tag{3}$$

where $P(t)$ is the output power, $g(t)$ and $q(t)$ are the intensity gain and saturable loss coefficients per cavity round trip, respectively, T_R is the cavity round-trip time, E_L is the saturation energy of the EDF (9.1 dBm $\times \tau_L$), τ_L is the upper-state lifetime of the EDF (9 ms), E_A is the saturation energy of the graphene SA ($\ll$1 pJ), τ_A is the relaxation time of the absorber ($\sim$2 ps), g_0 is the small-signal gain coefficient (0.8), q_0 is the small-signal loss coefficient (number of graphene layers $\times$ 2.3 %), E_I is the saturation energy of the EDF with respect to the injection power $P_i(t)$, and $\epsilon f(g)$ represents the small contributions to the intensity made by spontaneous emission.

3 Results

For the simulations, we used the Runge–Kutta methods iteratively within a standard delay differential equation (DDE) solver in MATLAB. Figure 2 shows the input spikes $P_i(t)$ that modulate the gain of the excitable laser (top) and the laser's intra-cavity power $P(t)$, with the state variables: gain $g(t)$, and absorption $q(t)$ (bottom). Each excitatory pulse increases the carrier concentration within the gain region by an amount proportional to its energy—gain enhancement. Enough excitation results in an excursion from equilibrium and a spike in power as a result of the saturation of the absorber to transparency, after which a relative *refractory period* occurs during which the pump current settles the system back to the 0-power attractor with fast recovery of $q(t)$ and the slow recovery of $g(t)$ to their equilibrium values. Insets (on right) show the different topologies of phase space that can occur as the physical parameters (such as current, length of cavity, absorption, etc.) are varied. We desire excitability, which occurs in the second phase portrait (outlined in red). Excitability that follows the behavior prescribed by the outlined phase portrait is simulated on left, with enough input perturbations ΔG resulting in the firing of a pulse, followed by a recovery period.

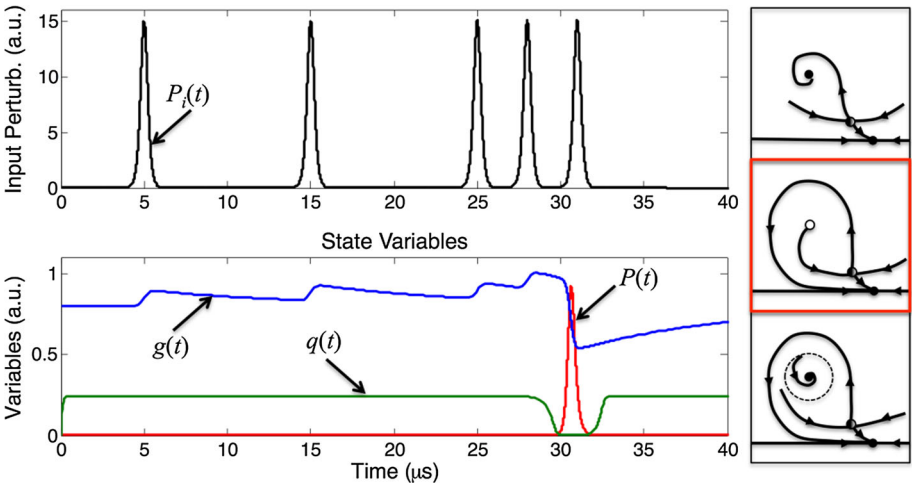

Fig. 2 Simulation results of the graphene Q-switched excitable laser

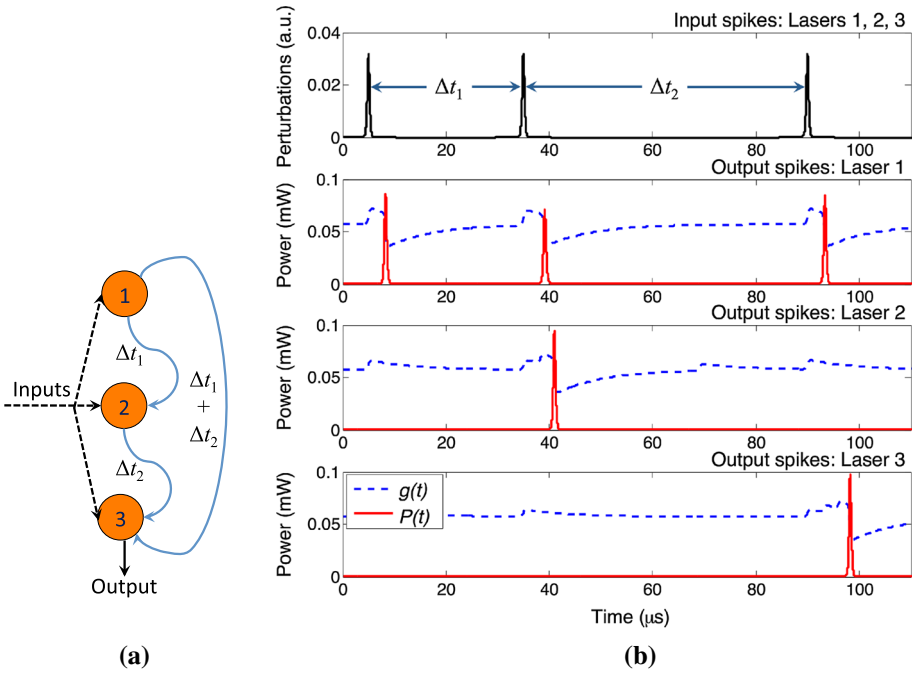

Fig. 3 **a** Schematic of a three-laser circuit to recognize specific spatio-temporal bit patterns. **b** Simulation of the spatio-temporal recognition circuit

In Fig. 3a, we construct a simple three unit pattern recognition circuit of our excitable lasers with carefully tuned delay lines, where each subsequent laser in the chain requires stronger perturbations to fire. Since weighing and delaying are both linear operations, they can be implemented optically with passive devices like attenuators and tunable delay lines. The resulting simulation is depicted in Fig. 3b along with the output powers of laser 1–3

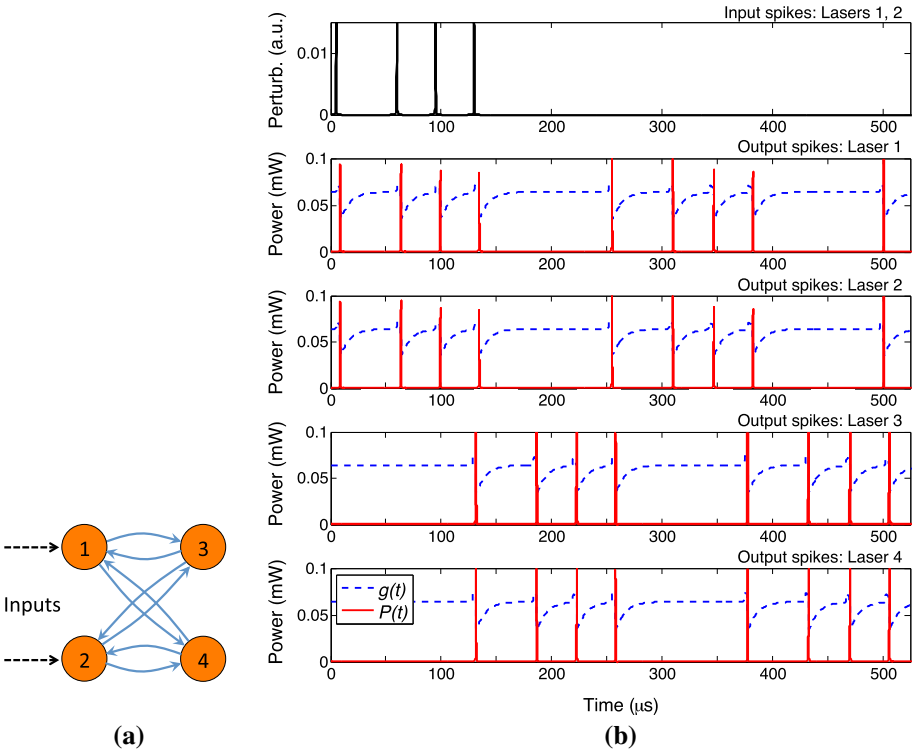

Fig. 4 **a** Schematic of a four-laser circuit forming synfire chains. **b** Simulation of the synfire chain circuit

and the scaled gain variable. Three excitatory inputs separated sequentially by $\Delta t_1 = 30\,\mu s$ and $\Delta t_2 = 55\,\mu s$ are incident on all three units. The third laser is configured only to fire if it receives pulses from the input and from the other two lasers simultaneously. The system therefore only reacts to a specific spatio-temporal bit pattern. This simple demonstration of temporal logic implies that a network of such excitable lasers are capable of categorization and decision making.

A key feature of a hybrid analog-digital system such as a spiking neural networks is that many analog nodes can process in a distributed and redundant way to reduce noise accumulation (Nahmias et al. 2013a). Recruiting a number of excitable lasers to accomplish the same computation is an effective and simple way of reducing spike error rates. Figure 4a shows a demonstration of a simple four-laser circuit forming synfire chains with connection delays of $135\,\mu s$. Recursion allows the synfire chain to possess hysteric properties. Once the spike pattern is input into the system as excitatory inputs injected simultaneously into the first two lasers, it is continuously passed back and forth between each set of two nodes. The spatiotemporal bit pattern persists after several iterations and is thereby stored in the network as depicted in Fig. 4b.

4 Conclusion

We have proposed and simulated a novel excitable laser employing passively Q-switching with a graphene SA for spike processing. Such an excitable system has recently been theo-

retically shown to behave analogously to a spiking neuron (Nahmias et al. 2013a, b), opening up applications for biologically-inspired cortical algorithms for high performance computing and adaptive control. Excitable lasers can also play an important role in pulse thresholding, regeneration, reshaping, and signal integrity for processing (Shastri et al. 2013b; Tait et al. 2013). The potential of excitable lasers to perform temporal logic grants the capacity for complex, ultrafast categorization and decision-making (Tait et al. 2014; Nahmias et al. 2013a). The current fiber-based system, while lacking scalability, is dynamically analogous to much smaller, integrated systems using deposited graphene absorbers. Thus, this model is useful for investigating dynamical properties and non-idealities (i.e. noise accumulation) using this easy-to-handle macroscopic demonstration to test basic network functionality. Ongoing research on graphene microfabrication may soon make it a standard technology accessible in integrated laser platforms. Pairing this technology with synaptic time dependent plasticity—a spike-based learning algorithm recently demonstrated in optics (Fok et al. 2013)—such networks could potentially be useful for applications including sequence learning and spike-pattern cluster analysis.

References

Barbay, S., Kuszelewicz, R., Yacomotti, A.M.: Excitability in a semiconductor laser with saturable absorber. Opt. Lett. **36**(23), 4476–4478 (2011)

Bonaccorso, F., Sun, Z., Hasan, T., Ferrari, A.: Graphene photonics and optoelectronics. Nat. Photon. **4**(9), 611–622 (2010)

Dubbeldam, J.L.A., Krauskopf, B., Lenstra, D.: Excitability and coherence in lasers with saturable absorber. Phys. Rev. E **60**(6), 6580–6588 (1999)

Fok, M.P., Tian, Y., Rosenbluth, D., Prucnal, P.R.: Pulse lead/lag timing detection for adaptive feedback and control based on optical spike-timing-dependent plasticity. Opt. Lett. **38**(4), 419–421 (2013)

Krauskopf, B., Schneider, K., Sieber, J., Wieczorek, S., Wolfrum, M.: Excitability and self-pulsations near homoclinic bifurcations in semiconductor laser systems. Opt. Commun. **215**(46), 367–379 (2003)

Maass, W., Bishop, C.M.: Pulsed Neural Networks. MIT Press, Cambridge, MA (1999)

Nahmias, M.A., Shastri, B.J., Tait, A.N., Prucnal, P.R.: A leaky integrate-and-fire laser neuron for ultrafast cognitive computing. IEEE J. Sel. Topics Quantum Electron. **19**(5), 1800,212 (2013a)

Nahmias, M.A., Tait, A.N., Shastri, B.J., Prucnal, P.R.: An evanescent hybrid silicon laser neuron. In: Proceedings of IEEE Photonics Conference (IPC), Seattle, WA, pp. 93–94 (2013b)

Sarpeshkar, R.: Analog versus digital: extrapolating from electronics to neurobiology. Neural Comput. **10**(7), 1601–1638 (1998)

Shastri, B.J., Nahmias, M.A., Tait, A.N., Tian, Y., Fok, M.P., Chang, M.P., Wu, B., Prucnal, P.R.: Exploring excitability in graphene for spike processing networks. In: Proceedings of Numerical Simulation of Optoelectronic Devices (NUSOD), Vancouver, BC, pp. 83–84 (2013a)

Shastri, B.J., Nahmias, M.A., Tait, A.N., Tian, Y., Wu, B., Prucnal, P.R.: Graphene excitable laser for photonic spike processing. In: Proceedings of IEEE Photonics Conference (IPC), Seattle, WA, pp. 1–3 (2013b). doi:10.1109/IPCon.2013.6656424

Spühler, G., Paschotta, R., Fluck, R., Braun, B., Moser, M., Zhang, G., Gini, E., Keller, U.: Experimentally confirmed design guidelines for passively Q-switched microchip lasers using semiconductor saturable absorbers. J. Opt. Soc. Am. B **16**(3), 376–388 (1999)

Tait, A.N., Shastri, B.J., Fok, M.P., Nahmias, M.A., Prucnal, P.R.: The DREAM: an integrated photonic thresholder. J. Lightw. Technol. **31**(8), 1263–1272 (2013)

Tait, A.N., Nahmias, M.A., Tian, Y., Shastri, B.J., Prucnal, P.R.: Photonic neuromorphic signal processing and computing. In: Naruse, M. (ed.) Nanophotonic Information Physics, Nano-Optics and Nanophotonics, pp. 183–222. Springer, Berlin (2014). doi:10.1007/978-3-642-40224-1_8

Vandoorne, K., Dierckx, W., Schrauwen, B., Verstraeten, D., Baets, R., Bienstman, P., Van Campenhout, J.: Toward optical signal processing using photonic reservoir computing. Opt. Exp. **16**(15), 11,182–11,192 (2008)